J. of Cardiovasc. Trans. Res.
DOI 10.1007/s12265-014-9563-7

Cardiac Electrical Activity in a Genomically "Humanized" Chromogranin A Monogenic Mouse Model with Hyperadrenergic Hypertension

Nagendu B. Dev · Saiful A. Mir · Jiaur R. Gayen · Jawed A. Siddiqui · Maja Mustapic · Sucheta M. Vaingankar

Received: 21 March 2014 / Accepted: 6 April 2014

Abstract The prohormone chromogranin A (CHGA) is ubiquitously found in vesicles of adrenal chromaffin cells and adrenergic neurons, and it is processed to the hypotensive hormone peptide catestatin (CST). Both CHGA and CST regulate blood pressure and cardiac function. This study addresses their role in cardiac electrical activity. We have generated two genomically "humanized" transgenic mouse strains (Tg31*CHGA*+/+; *Chga*−/− (Hum*CHGA*31) and Tg19*CHGA*+/+; *Chga*−/− (Hum*CHGA*19)) with varied *CHGA* expression and the ability to rescue the *Chga*−/− phenotype (hypertensive, hyperadrenergic with dilated cardiomyopathy). The normotensive Hum*CHGA*31 mice express CHGA at levels comparable to wild-type. In contrast, the hypertensive Hum*CHGA*19 mice have low levels of CHGA. EKG recordings revealed that the QT interval, R-amplitude, and QRS time-voltage integral are markedly longer in Hum*CHGA*19 compared to wild-type and Hum*CHGA*31 mice. These differences are accompanied by increased heart rate and QT variability, indicating that ventricular assault happens in a status of low levels of circulating CST.

Keywords Chromogranin A · Catestatin · Genomically "humanized" *CHGA* mice · QT variability · Cardiomyopathy index · Ventricular power-frequency spectra

Abbreviations and Acronyms

au	Arbitrary unit
BP	Blood pressure
Chga	Mouse chromogranin A gene
CHGA	Human chromogranin A gene
CHGA	Chromogranin A protein
CI	Statistical confidence interval
CST	Catestatin
cv	Coefficient of variation=[standard deviation/sample mean]
DBP	Diastolic BP
DCM	Dilated cardiomyopathy
EKG	Electrocardiography
HR	Heart rate
Hum*CHGA*19	Genomically "humanized" transgenic mice Tg19*CHGA*+/+*Chga*−/−
Hum*CHGA*31	Genomically "humanized" transgenic mice Tg31*CHGA*+/+*Chga*−/−
HRV	Heart rate variability
PQ	Atrio-ventricular conduction time
QRSd	Duration of QRS-wave complex
QTb	Bazett-corrected QT interval
QTb/PQ	Cardiomyopathy index
QTu	Uncorrected QT interval
QTVI	QT variability index
RR	Sinus cycle length

Editor-in-Chief Jennifer L. Hall oversaw the review of this article

Nagendu B. Dev and Saiful A. Mir contributed equally to this work.

Electronic supplementary material The online version of this article (doi:10.1007/s12265-014-9563-7) contains supplementary material, which is available to authorized users.

N. B. Dev · S. A. Mir · J. A. Siddiqui · M. Mustapic · S. M. Vaingankar (✉)
Department of Medicine, University of California at San Diego, La Jolla, CA, USA
e-mail: svaingankar@ucsd.edu

J. R. Gayen
CSIR-Central Drug Research Institute, Lucknow, India

Published online: 13 May 2014

SBP	Systolic BP
WT	Wild-type mice

Introduction

The prohormone chromogranin A (CHGA) is a member of the granin family of proteins and is sequestered in granules of the adrenal medulla and postganglionic sympathetic axons along with catecholamines and calcium [1–3]. It plays a crucial role in biogenesis of the secretory granules itself, interacts with several proteins in the regulated secretory pathway, and recruits cytosolic proteins to the membrane of granules [4, 5]. The pro-protein CHGA is processed to generate several biologically active peptide fragments including the neuropeptide catestatin (CST). CST exerts sympatho-inhibitory effects by weakening nicotinic cholinergic pathway, thereby controlling blood pressure (BP) and heart rate (HR) [6]. CHGA has been reported to have significant dose-dependent myocardial contractile (inotropic), relaxing (lusitropic), and coronary (vasomotive) effects on the rat heart performance [7]. Administering CST in reperfusion reduces post-ischemic myocardial damages and dysfunction, suggesting a cardioprotective function for CST [8]. In humans, the CHGA expression is heritable and elevated in essential hypertension [9, 10]. Plasma concentration of CST is diminished both in patients with hypertension and their normotensive offspring at a genetic risk of developing the disease [11–13]. Heritability of CST has also been established in a genome-wide twin study with the hypertensive subjects displaying elevated CHGA coupled with diminished CST [14]. Thus, CST levels in plasma may be an important "intermediate" phenotype in analysis of genetic risk for human hypertension. The *Chga* null mice lack CST and as a result have elevated circulating catecholamines and are hypertensive, with decreased baroreflex sensitivity [15]. Echocardiography measurements show cardiomyopathy and ventricular hypertrophy [16]. In sedated *Chga*−/− mice, the heart rate variability (HRV), an index of autonomic function, is highly compromised and partially restored by CST replacement [17]. Meng et al. have observed elevated plasma CST post-acute myocardial infarction, leading to inhibition of catecholamine release and association with progressive ventricular remodeling [18].

Elevated circulating catecholamines elicit changes in ventricular electrical conduction time, as exemplified in diseases like idiopathic mitral valve prolapse [19]. A prolonged QT interval observed in the electrocardiogram (EKG) profile signifies a delay in the ventricular repolarization phase, which renders the heart vulnerable to ischemic damage (IHD) or malignant arrhythmias such as torsade de pointes or ventricular tachycardia. QT-interval prolongation has also been associated with lowered ventricular fibrillation threshold and occurrence of sudden cardiac death [20]. Ventricular instability in humans is often a feature of dilated (DCM) and hypertrophic cardiomyopathy.

We have previously described two genomically "humanized" *CHGA* mouse models, expressing sufficient (Hum*CHGA*31, normotensive) vs. insufficient (Hum*CHGA*19, untreated hypertensive) levels of human CHGA that mimic the variability in human chromogranin A gene (*CHGA*) expression observed in the human population [21]. These transgenic models stably express the human *CHGA* gene in the mouse *Chga* knockout (*Chga*−/−) background. The variation in *CHGA* expression in these mice results in variable release of adreno-medullary catecholamines. The Hum*CHGA*31 have circulating human CHGA and catecholamine levels comparable to wild-type (WT) mice. In contrast, the Hum*CHGA*19 have 14-fold lower circulating human CHGA accompanied by elevated plasma catecholamine. Thus, the Hum*CHGA*19 mice have elevated systolic BP (SBP) and diastolic BP (DBP) [21].

We hypothesized that due to low levels of CHGA, the Hum*CHGA*19 mice would have attenuated levels of the hypotensive CST peptide resulting in enhanced ventricular vulnerability. Our assumption was that both the "humanized" *CHGA* mouse models with differential CHGA expression and ability to "rescue" the hypertensive, hyperadrenergic *Chga* null phenotype would reveal the involvement of CHGA in cardiac electrical activity. We measured the human CST levels in plasma of these mice and performed EKG to determine whether circulating CHGA and CST levels correlate with ventricular depolarization especially Bazett-corrected repolarization time (QTb) and atrio-ventricular conduction time (PQ) along with QTb/PQ changes (cardiomyopathy index as defined by Steare) [22]. The main finding of this study is that CHGA and, therefore, CST levels influence BP and cardiac electrical activity. Compared to Hum*CHGA*31, the Hum*CHGA*19 mice have low levels of plasma CHGA and CST, a scenario comparable to the hypertensive humans. Hum*CHGA*19 mice display prolonged QTb, compressed sinus cycle length (RR) variability, and increased duration of QRS-wave complex (QRSd) coupled with decreased PQ resulting in compromised cardiac function, compared to Hum*CHGA*31 with normal CST levels.

Materials and Methods

Genomically "Humanized" Transgenic Mouse Models

The genomically "humanized" mice were generated by bacterial artificial chromosome transgenesis as detailed earlier [21, 16]. Both transgenic strains have the complete ~12 kb

human *CHGA* transgene and the flanking native human chromosome 14 sequence. The founder Tg19*CHGA*+/−; *Chga*+/+ had ~42 kb upstream and ~19 kb downstream flanking sequence, whereas Tg31*CHGA*+/−; *Chga*+/+ had ~44 kb upstream and 155 kb downstream sequence. These mice were crossed with *Chga*−/− mice and subjected to brother–sister mating for ~10 generations to generate the transgenic lines lacking the mouse *Chga* alleles and having diploid copies of the transgene Tg19*CHGA* or Tg31*CHGA*. Thus, the WT mice express mouse *Chga*, and both "humanized" strains express exclusively the human *CHGA* transgene. All three strains of mice have the identical mixed-background (50 % C57BL/6:50 % 129/SvJ).

Animal Husbandry

Mice were kept under pathogen-free conditions, maintained on a normal murine chow-diet, and allowed to have water ad libitum. Experiments were carried out in accordance with the Institutional Animal Care and Use for scientific purposes and with the guidelines adopted by the National Institutes of Health. All possible steps were taken to avoid animals' suffering during the experiment. The three groups of mice (age 28.4–29.1 weeks) of either sex were used in the study.

Measurement of Blood Pressure, Plasma Catestatin, and Heart Weight:Body Weight Ratio

The previously described non-invasive tail-cuff method was used to measure BP of all three strains of mice for 5 days [21]. SBP and DBP data were subjected to statistical one-way ANOVA with multiple-comparison post hoc tests using SPSS Statistics software from IBM. The BP was also measured in Hum*CHGA*31and WT mice using telemetric DSI transmitters. Telemetry signals relayed the data to a signal processor (DataQuest A.R.T. Gold, version 2.3; Data Sciences International) connected to a desktop personal computer (Hewlett-Packard, Portland, OR, USA). After the implantation surgery, the animals were rested for 10 days for normalization of the diurnal pattern of BP, before recording BP in these conscious mice. The data obtained from both the procedures were compared by the Student *t* test.

Plasma samples were collected from "humanized" mice euthanized by deep anesthesia with isoflurane and stored at −70 °C until CST was assayed using the CST (human specific) EIA kit from Phoenix Pharmaceutical Inc. (CA, USA) according to the manufacturer's instructions.

To evaluate cardiac hypertrophy morphometrically, hearts were excised from the euthanized mice, weighed, and used to determine the ratio of heart weight (mg) and body weight (g) [23, 24].

Electrophysiology

EKG recordings were carried out in conscious mice at an ambient temperature of 20–22 °C between the hours of 10:00–15:00 to minimize circadian influences. EKG complexes were sampled from recordings with clearly defined onset and termination signals. Surface EKG was performed using stainless steel micro needles (Grass instruments, Quincy, MA, USA) strapped to the limbs of the mouse. The mouse was transferred to a conventional laboratory murine cage in which it could move freely. Experiments were carried out in a noise-free environment with ambient light. All moving artifacts in the EKG signals were filtered out during analysis. Lead II EKG signals were sampled at a rate of 2 kHz and digitized with a 16-bit analog-to-digital converter (Powerlab 8/30, AD instruments). Signal data were stored directly onto a hard disk for post-processing. The mice were allowed to become accustomed to the recording environment for ~10 min prior to storing of the EKG data for analysis. Only data from continuous recording of 20–30 EKG signals was used for analysis. The RR intervals in the EKG were extracted using a detection algorithm based on thresholding. All extreme (<70 and >300 ms) RR intervals were excluded from analysis. Atrial and ventricular wave complexes were analyzed with a scanning speed of 500 mm/s. EKG data were analyzed from quasi-stationary conditions of RR and QT time-series, necessary for variability analysis from a standpoint of signal-processing. The QRS duration was measured from the onset of the Q wave to the peak negative deflection of the S wave (this is in contrast to return of S wave to the isoelectric baseline in human designated as QRS duration). QT-interval durations and other wave complexes were determined from signal averaged of considerable number of lead II EKG signal (SAEKG) or manually evaluated. EKG waves are defined as the positions where the signal derivative changes its sign. Each QT interval was measured from the beginning of the QRS complex up to the end point of the T wave, defined as the intersection of the steepest slope of the descending T wave and the isoelectric line. Original QT values were corrected (QTb) using the Bazett formula [25]. In humans, prolonged corrected QT is defined as a QTb interval >440 ms [20]. Typically, the EKG parameters in mice are 7 to 8 fold different compared to humans. For example, the heart rate in humans is 70–80 beats/min and in mice, 550 beats/min; the QRS duration in humans is 0.12–0.2 s and in mice, 10–15 ms [26, 27]. Therefore, we considered a QTb value >65 ms as prolonged QTb in mice. Influence of HR on QTb was analyzed statistically. QRS-wave data were subjected to power-frequency analysis following sampling at

FFT256 with 50 % overlap and a Welch-correction filter. Variability in QT intervals is recognized as an assessment of temporal myocardial repolarization lability. Therefore, in all strains of mice, we evaluated beat-to-beat ventricular repolarization variability quantified by the QT variability index (QTVI), according to Berger et al. [28].

Statistical Analysis

Data were evaluated in Instat software (Graphpad, San Diego, CA, USA) and subjected to one-way ANOVA analysis, following normality and Kolmogorov–Smirnov tests for Gaussian data distribution. These data were reported as mean differences among the test groups and p values generated after application of Mann–Whitney U test, Kruskal–Wallis test, or Welch-corrected test. Relationships between variables were evaluated with Spearman or Pearson rank correlation tests. Post hoc multiple-comparison procedure of Tukey–Krammer honestly significant difference (HSD) test was used to analyze the difference between strain means, if applicable. When testing the effects of CHGA on multiple correlated traits, we estimated the false discovery rate (FDR) to minimize false negative results while maximizing true positive results, using the Excel calculator of FDR from a distribution of p values at http://www.rowett.ac.uk/~gwh/fdr.html.

Results

Blood Pressure and Circulating CST in "Humanized" *CHGA* Mice

The Hum*CHGA*19 mice used in this study displayed higher SBP (~17–19 mmHg) and DBP (~17–22 mmHg) compared to Hum*CHGA*31and WT mice (Fig. 1a), consistent with our previously published results [21]. The BP was measured by tail-cuff method in mice, prior to EKG recordings. Comparison using statistical Student t test of BP data obtained by both indirect tail-cuff and direct telemetric measurements for WT (SBP, p=0.984; DBP, p=0.163) and Hum*CHGA*31 (SBP, p=0.119, DBP p= 0.278) mice confirmed that results from both methods were similar. Hypertensive patients display attenuated levels of CST [11–13]. Therefore, a competitive enzyme immunoassay was employed to detect the circulating levels of human CST and/or related peptides in both the strains of "humanized" *CHGA* mice. The hypertensive Hum*CHGA*19 mice had diminished CST (0.5-fold) compared to Hum*CHGA*31mice (Fig. 1b). The heart weight (mg):body weight (g) ratio of the Hum*CHGA*19 mice was not significantly (p=0.078) higher from that of Hum*CHGA*31 mice, suggesting that cardiac hypertrophy is not an overriding attribute in differences between the strains (Fig. 1c; Supplementary Fig. 1). Therefore, to assess the implications of CHGA and CST expression

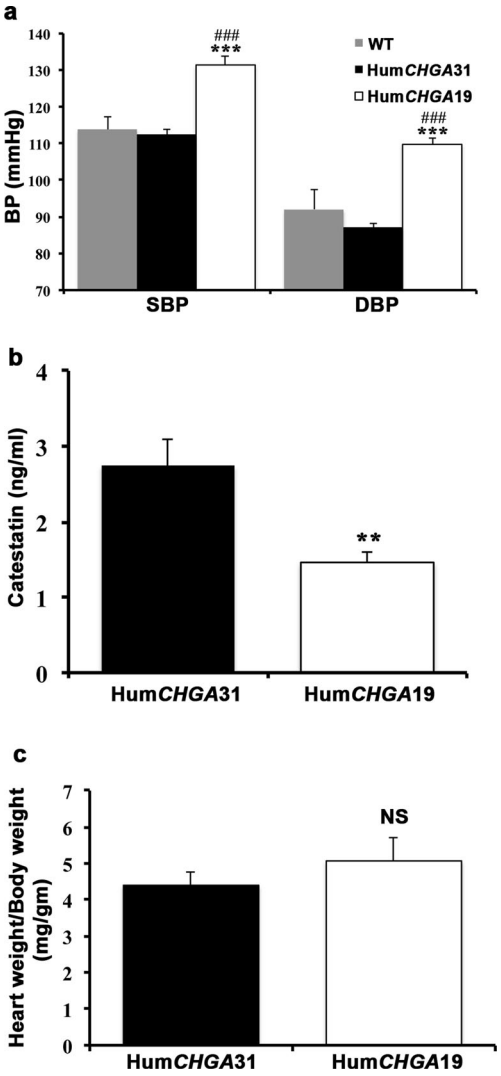

Fig. 1 The BP of genomically "humanized" *CHGA* mice correlated with circulating CST levels: The "humanized" transgenic mice express the human *CHGA* gene, and their BP was measured along with that of the WT mice. In these "humanized" *CHGA* mice, circulating levels of the human CST was also measured. **a** Elevated BP in Hum*CHGA*19 mice: The SBP was significantly different between groups of mice as determined by one-way ANOVA with multiple-comparison post hoc tests (p<0.0001). Specifically, Hum*CHGA*19 had higher SBP compared to WT ($^{\#\#\#}p$=0.0004) and Hum*CHGA*31 (***p=0.00005). DBP also varied significantly in the Hum*CHGA*19 mice compared to Hum*CHGA*31 and WT mice (p<0.0001). In Hum*CHGA*19 mice, the DBP was elevated compared to both WT and Hum*CHGA*31 ($^{\#\#\#}$, ***p=0.00001). **b** The plasma concentration of the hypotensive CST peptide is inversely correlated with BP: Circulating CST was measured in the mouse plasma using a competitive ELISA that quantitates human CST and thus expression of the transgene in the "humanized" *CHGA* mouse models. The Hum*CHGA*31 mice exhibit normal BP and had almost twice as much CST as the hypertensive Hum*CHGA*19 mice (**p<0.007). **c** Heart weight (mg):body weight (g) ratio is not significantly different between both the transgenic strains

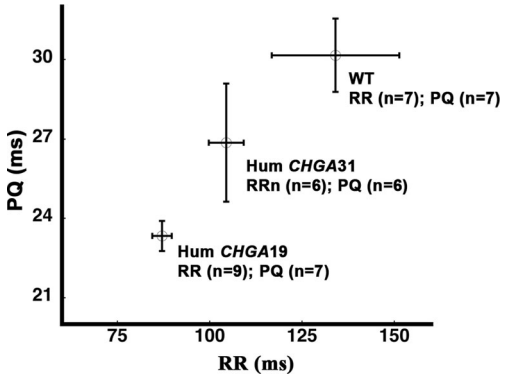

Fig. 2 Dependence of atrio-ventricular conduction time (PQ) on sinus cycle length (RR): The EKG profiles of the WT and "humanized" transgenic Hum*CHGA*19 and Hum*CHGA*31 mice revealed dependence of PQ conduction time on RR. Statistical analysis did not reveal any significant differences ($p>0.05$) in the PQ/RR relationship among the three groups. The number of mice used in the analysis is indicated by "*n*"

levels in cardiac electrical activity, EKG was performed on these mice.

Atrio-Ventricular Conduction (PQ Interval)

The atrio-ventricular conduction time (PQ) is an estimate of AV node function that measures the duration for the electrical impulse to travel from the SA node through the AV node to the ventricles. At rest, PQ generally decreased with decreased sinus cycle length (RR). However, at a given RR interval, inter-subject variability was observed in the PQ interval in all three groups (Fig. 2). Inter-subject variability is a function of the subject's pre-existent vagal and sympathetic tone. PQ conduction times and their association with sinus cycle length data are presented in Table 1. The PQ values in Hum*CHGA*19 were lower compared to WT and Hum*CHGA*31 mice. The sinus cycle lengths were not significantly different between Hum*CHGA*31 and WT. However, these differences were significant between Hum*CHGA*19 vs. WT and between Hum*CHGA19* vs. Hum*CHGA*31. The cardiac parameters measured in this study (Table 1) agree with those observed in WT mice by Xing et al. [29].

The percentage of the atrio-ventricular conduction time to the sinus cycle length (PQ/RR) was found to be around 25 % in the awake WT mice and was totally unaffected by transgenesis (both Hum*CHGA*19 and Hum*CHGA*31). A slope of PQ to RR, tan $\theta \approx 45°$ in Fig. 2, suggests that mice in each of the studied group make an effort to optimize energy efficiency via adequate systolic and diastolic volume with increased or decreased sinus rhythm. Therefore, there are no apparent physiological defects in the atrio-ventricular conduction among the tested mice. An inverse relationship of PQ conduction to RR in human has been described earlier [30] and seems to hold true for mice investigated in the present study. PQ conduction time data for WT mice in this study resemble the earlier report of mice intracardiac electrogram [31].

Non-parametric Kruskal–Wallis with Dunn's multiple-comparison test revealed a significant difference in heart rates (HR = [1/RR]) among WT and Hum*CHGA*31 vs. Hum*CHGA*19 (Table 1). Analysis of our preliminary (unpublished) experimental data also revealed that all-time domain parameters of HRV, e.g., SDNN, RMSSD, and NN6

Table 1 Atrio-ventricular conduction time (PQ) and its dependence on sinus cycle length (RR)

	WT	Hum*CHGA*31	Hum*CHGA*19	ANOVA (*F* and *p* values)
n	7	5	7	–
PQ (ms)	30.16±1.39	26.86±2.23	23.33±0.57	$F=39.08$ $p<0.001$ (FDR $p<0.001$)
PQ_{CI} (ms)	27.0–33.31	21.33–32.41	22.04–24.63	–
n	7	6	9	–
RR (ms)	134.09±17.28	104.50±4.73	87.09±2.64	$F=42.39$ $p<0.001$ (FDR $p<0.001$)
RR_{CI} (ms)	94.93–173.24	93.40–115.60	81.35–92.83	–

The atrio-ventricular conduction values (PQ) in Hum*CHGA*19 mice were significantly different from WT ($p<0.001$) and Hum*CHGA*31 ($p<0.01$) mice. Sinus cycle lengths (RR) did not significantly differ between Hum*CHGA*31 and WT ($p>0.05$). However, the RR values following a Welch-correction factor (PQ_{CI} and RR_{CI}), varied significantly between Hum*CHGA*19 vs. WT ($p<0.02$, $p>0.01$) and between Hum*CHGA*19 vs. Hum*CHGA*31 ($p<0.005$). The PQ and RR values are represented as mean values±standard deviation. The range in PQ_{CI} and RR_{CI} values are shown. The number of experimental animals is represented in row "*n*". Shown in the last column are the *F* and *p* values of the data analyzed by one-way analysis of variance (ANOVA), followed by the Bonferroni post hoc test when the *p* value was <0.05, to measure the difference between groups

FDR false discovery rate

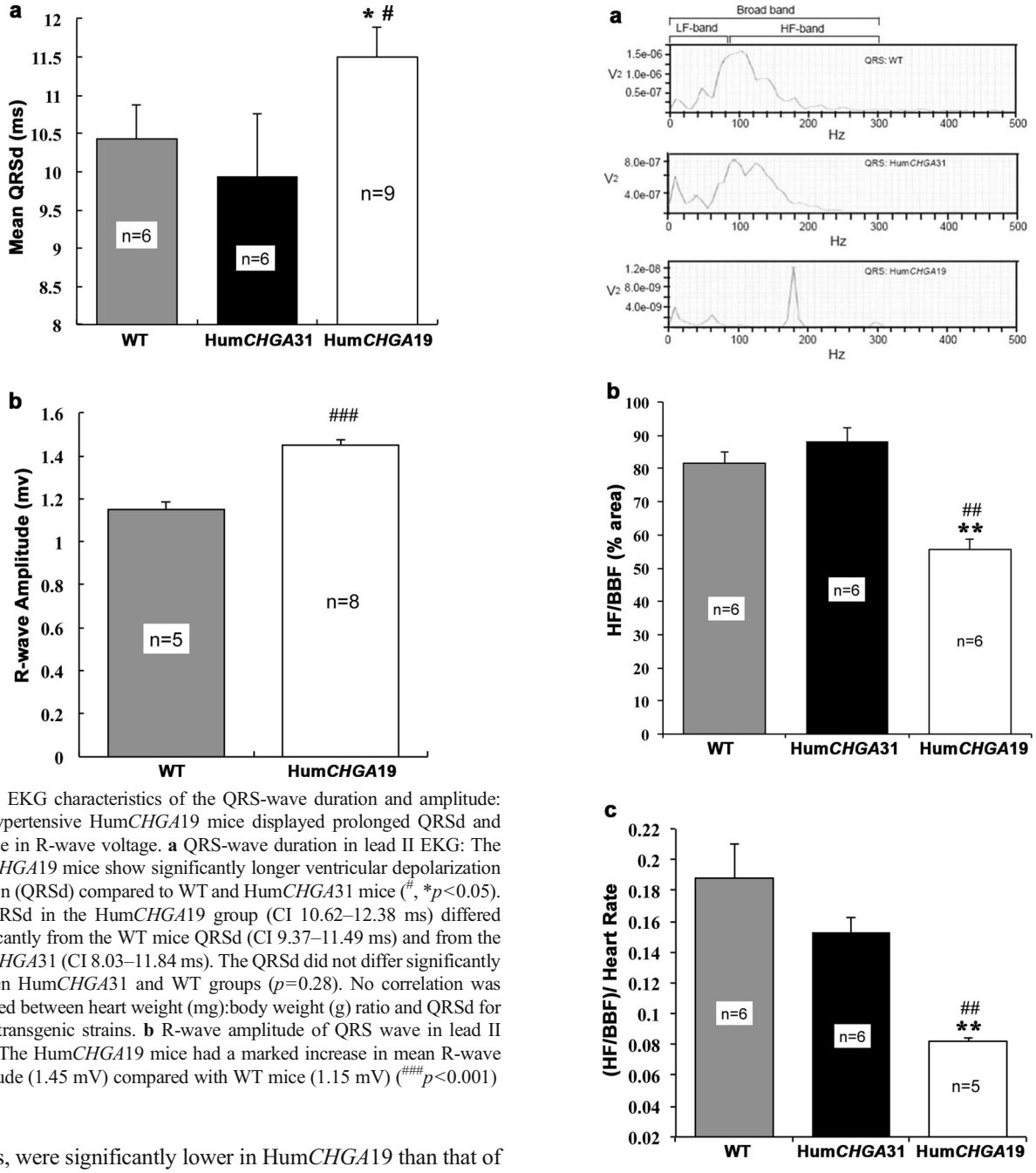

Fig. 3 EKG characteristics of the QRS-wave duration and amplitude: The hypertensive Hum*CHGA*19 mice displayed prolonged QRSd and increase in R-wave voltage. **a** QRS-wave duration in lead II EKG: The Hum*CHGA*19 mice show significantly longer ventricular depolarization duration (QRSd) compared to WT and Hum*CHGA*31 mice ($^{\#}$, *$p<0.05$). The QRSd in the Hum*CHGA*19 group (CI 10.62–12.38 ms) differed significantly from the WT mice QRSd (CI 9.37–11.49 ms) and from the Hum*CHGA*31 (CI 8.03–11.84 ms). The QRSd did not differ significantly between Hum*CHGA*31 and WT groups ($p=0.28$). No correlation was observed between heart weight (mg):body weight (g) ratio and QRSd for either transgenic strains. **b** R-wave amplitude of QRS wave in lead II EKG: The Hum*CHGA*19 mice had a marked increase in mean R-wave amplitude (1.45 mV) compared with WT mice (1.15 mV) ($^{\#\#\#}p<0.001$)

values, were significantly lower in Hum*CHGA*19 than that of WT and Hum*CHGA*31.

Ventricular Depolarization Time (QRS Duration)

Measurements of ventricular depolarization time and R-wave amplitude are shown in Figs. 3a and 3b, respectively. QRS duration (QRSd) of ventricular complex was larger in the Hum*CHGA*19 group and differed significantly from the QRSd of WT and the Hum*CHGA*31 mice. In summary, the values of QRSd are Hum*CHGA*19 > WT > Hum*CHGA*31. In Hum*CHGA*19 along with an increase in QRSd, R-wave amplitude in QRS complex also increased (Fig. 3b). However, no correlation was observed between QRSd and heart weight:body weight ratios for both strains of mice (the Hum*CHGA*31 $r=-0.19$, two-tailed $p=0.76$; and the Hum*CHGA*19 $r=-0.22$, $p=0.72$).

QRS-wave data were also segmented into low- (LF) and high-frequency (HF) spectral band for possible differentiation of the ventricular power structure among the studied groups. Frequency range was selected on the basis of earlier experiments in mice [32]. However, we observed massive power loss that occurred in all experimental groups and reached almost null power at frequencies >300 Hz. Therefore, we

◀ **Fig. 4** The HF-band power segment of the BBF in the QRS wave is reduced in Hum*CHGA*19 mice: The broadband frequency area (BBF) of the QRS-wave segments was further analyzed. The BBF comprises the sympathetic LF (low frequency) and the parasympathetic HF (high frequency) areas, indicative of efferent activity at the sinus node. **a** An illustration of power frequency of QRS-wave plot: These plots were derived from actual experiments. Note in Hum*CHGA*19 mice, the frequency shift of peak power in the HF range along with a decrease in total power across the frequency range. **b** The QRS wave segmented into average percentage of time spent in HF: Percentage of HF (80–300 Hz) area in the total BBF in the QRS wave was significantly reduced in Hum*CHGA*19 mice compared to WT and Hum*CHGA*31 mice ($^{##}$, $^{**}p<0.01$). Analyzed data of the QRS spectra had the following characteristics: Hum*CHGA*19—BBF area, 0.52; 0–80 Hz, 0.21; 80–300 Hz, 0.31 (HF 59.61 % of BBF); Hum*CHGA*31—BBF area, 2.038; 0–80 Hz, 0.53; 80–300 Hz, 1.50 (HF 73.60 % of BBF); and WT—BBF area, 2.00; 0–80 Hz, 0.49; 80–300 Hz, 1.51 (HF 75.5 % of BBF). The area values are in arbitrary unit (au). **c** Influence of HR on the HF (80–300 Hz) part of BBF (0–300 Hz) spectral area: *Bar graph* shows that the fraction of HF area in the BBF of Hum*CHGA*19 significantly lowered as compared to mice in other groups, as the sinus cycle length decreases ($^{##}$, $^{**}p<0.01$)

chose 0–80 Hz as LF band, 80–300 Hz as HF band, and 0–300Hz in which 98 % power resides as broadband frequency (BBF) spectral band. A representation of QRS-wave power-frequency profile is presented in Fig. 4a. A conspicuous finding was that in the Hum*CHGA*19 group, HF peak power of QRS-wave spectrum narrowly centered around 150–200 Hz, whereas HF peak power in the Hum*CHGA*31 and WT mice showed a distinct leftward shift toward LF (<150 Hz). However, in the Hum*CHGA*31 and WT mice, the frequency span, over which peak power in the HF range occurred, was broader and not as narrow as observed in the Hum*CHGA*19 group. The QRS spectra were analyzed for all the three strains of mice, and their characteristics are presented in Fig. 4b. Statistical analysis via non-parametric ANOVA of the HF area in the QRS spectra showed that the average percentage of time spent in the HF in the BBF decreased as the RR decreased. Markedly so, it was evidenced in the

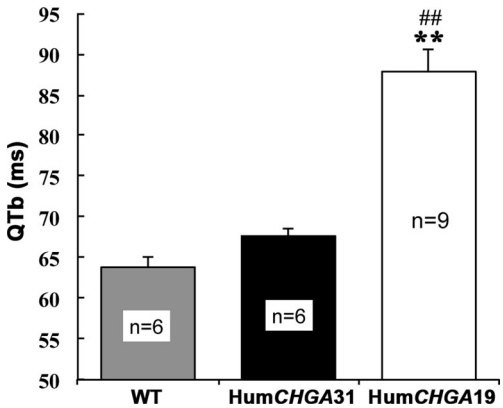

Fig. 5 Bazett-corrected QTb in mice: Note the significantly ($^{##}$, $^{**}p<0.01$) prolonged QTb (index of myocardial repolarization status) in Hum*CHGA*19 compared to WT and Hum*CHGA*31 mice

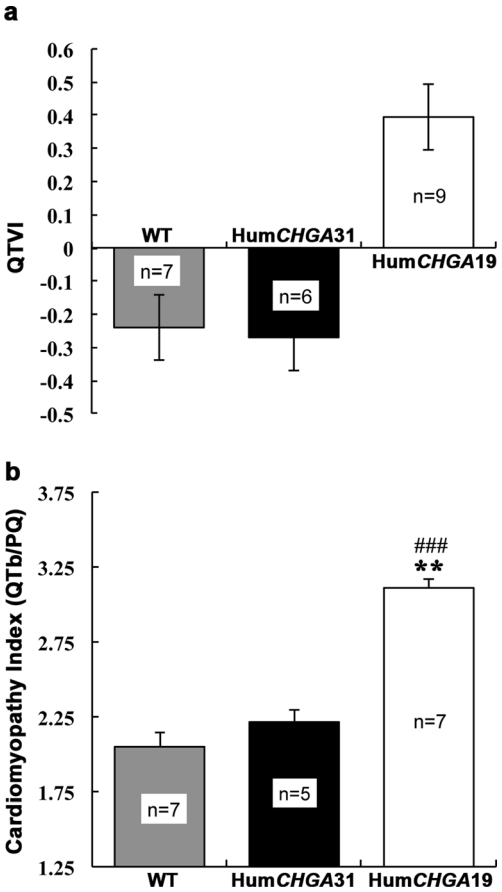

Fig. 6 Influence of *CHGA* gene expression on $\log_{10}$ QT variability index (QTVI) and cardiomyopathy index (QTb/PQ): From "humanized" and WT conscious mice, EKG signal was acquired in lead II configuration at a sampling rate of 2 kHz. **a** Elevated QTVI in Hum*CHGA*19 mice: Compared to Hum*CHGA*31 and WT mice, Hum*CHGA*19 have augmented beat-to-beat fluctuations in QT interval that are larger than normal and uncoupled from variations in HR. **b** Cardiomyopathy index (QTb/PQ): Significant increase in the QTb:PQ ratio in Hum*CHGA*19 was observed as compared to WT ($^{###}p<0.001$) and in the Hum*CHGA*31 mice ($^{**}p<0.01$), suggesting electrophysiological parallel of increased myopathy of cardiac muscles. However, the correlation between the hypertensive Hum*CHGA*19 strain's heart size and increased QTb/PQ was not significant ($p=0.082$)

Hum*CHGA*19 mice (Fig. 4c). In summary, percentage area of HF/BBF: Hum*CHGA*19 < WT < Hum*CHGA*31 and for area dependence on heart rate, [(HF/BBF)/HR]: Hum*CHGA*19 <Hum*CHGA*31 < WT.

Ventricular Repolarization Duration (QT Variability Index)

Coupling of heart rate (1/RR) and ventricular repolarization time (QT) in humans has been extensively described in the literature, albeit not without dispute. Therefore, we examined the association between these variables in WT mice, using the Bazett-correction of QT (QTb). The variables were statistically linear and not significantly deviated ($p>0.52$) from the linearity (Pearson correlation coefficient, $r=0.89$). Having

Table 2 Uncorrected QT (QTu) interval and sinus cycle length (RR)

	WT	Hum*CHGA*31	Hum*CHGA*19	ANOVA (*F* and *p* values)
n	6	6	9	–
RR interval (ms)	140.44±6.21	104.78±1.55	87.09±0.93	F=437.925 p<0.001 (FDR p<0.001)
QTu interval (ms)	23.26±0.24	21.62±0.23	24.07±0.39	–
RR (cv)	0.283	0.093	0.083	–
QTu (cv)	0.067	0.066	0.126	F=110.55 p<0.001 (FDR p<0.001)

The values of coefficient of variation (cv) of RR and uncorrected QT interval are calculated (100×standard deviation/average value). In Hum*CHGA*19 mice the QT (cv) is higher and fairly compressed in variability in the RR cycle length, compared to Hum*CHGA*31 and WT mice. "*n*" indicates the number of experimental mice in each group. The last column shows the *F* and *p* values of the one-way ANOVA

FDR false discovery rate

confirmed the validity of the Bazett formula in this series of experiments, the Bazett-correction (QTb) factor [QTb=(QTu/$RR^{1/2}$)] was applied to other mouse models as well. A graphic representation of the QTb values is shown in Fig. 5. WT and Hum*CHGA*31 mice maintained a significant positive linear relation of QTb and HR. In contrast, Hum*CHGA*19 QTb almost failed to follow changes in HR, and the relationship of these variables became non-significant (p>0.58). Heart rate and uncorrected QT interval (QTu) exhibited beat-to-beat variability among the studied groups and was apparent in the calculated values of coefficient of variation (cv, standard deviation/sample means).

QTVI is an indicator of cardiac repolarization lability and cardiac sympathetic function. The QTVI was significantly greater in Hum*CHGA*19 than in either Hum*CHGA*31 or WT mice as shown in Fig. 6a. Respective cv values in Hum*CHGA*31 and WT for HR were 0.097 and 0.304, and for QTb 0.067 and 0.137. In sharp contrast, the Hum*CHGA*19 mice had an extremely constrained HR cv value of 0.081and for QTb a value of 0.112, without any discernible relation with instantaneous HR. Differences in QTVI among the mice were also reflected in the parameters of QTb/PQ. Particularly, the mean PQ duration of 23 ms was distinctly lower in the Hum*CHGA*19 group, a reduction of over 23 and 15 % from the values obtained in the WT and Hum*CHGA*31, respectively. Similarly, corrected QT (QTb) value was markedly higher in Hum*CHGA*19, an increase of 38 and 28 % compared to WT and Hum*CHGA*31, respectively, and as a result, the magnitude of QTb/PQ (cardiomyopathy index) increased significantly in Hum*CHGA*19 (Fig. 6b). Again, the QTb:PQ ratio is not significantly correlated with heart weight:body weight ratio (Hum*CHGA*31 r=−0.36, p=0.55; Hum*CHGA*19 r=−0.83, p=0.08).

Discussion

The main findings of this study are that *CHGA* and thus CST expression levels are involved in fine-tuning of ventricular repolarization during QT interval. The BP responses obtained in mice with varying CHGA dosage and the data presented here suggest a critical role for sympathetic stimulation and catecholamine levels for supporting QT prolongation [33, 21]. The effect of sympathetic blockage on the QT:RR ratio has been demonstrated by pharmacological autonomic blockade experiments of Extramiana et al. [34]. In humans, QTb greater than >480 ms especially >500 ms has been reported to cause sudden cardiac death. Theoretically, in mice, this should correspond to a QTb value of >60 ms. In Hum*CHGA*19 mice, QTb values >60 ms was routinely observed, suggesting that these mice are susceptible to ventricular arrhythmia. In Hum*CHGA*19 mice, a dysfunction in cardiac performance occurs because the QT coefficients of variation (cv) values are higher and the RR cycle length variability fairly compressed, compared to Hum*CHGA*31 (Table 2).

In humans, the prolongation of QRS complex duration is regularly listed among electrocardiographic signs of left ventricular hypertrophy (LVH). QRSd has also been found to correlate with left ventricular mass [35]. Dunn et al. also reported progressively increased QRSd with progressive left ventricular hypertrophy in SHR rats [36]. These findings are in line with the observations of this study, in which prolonged QRSd is a unique feature in Hum*CHGA*19 mice and can be considered as a possible corollary to anatomical LVH. Earlier echocardiographic data of *Chga*−/− mice also indicated LVH [16]. The increase in R-wave voltage observed in Hum*CHGA*19 may tentatively be attributed to hypertrophic status of the ventricle. This is also similar to "LIFE" clinical

study that shows longer QRS- and QT-interval measures in the hypertensive population [37]. However, the Hum*CHGA*31 and Hum*CHGA*19 strains do not differ significantly in their heart weight:body weight ratios, and these ratios do not correlate with QRSd values or the cardiomyopathy index (QTb/PQ). Therefore, cardiac hypertrophy is not a dominant trait difference between strains. VanderBrink et al. found that HF band area of QRS depolarization wave in mice was 18-fold over that of human (55 vs. 3 %) and postulated that HF area might be positively related to the HR [31]. This interpretation is based on known HR differences across species (man vs. mice). Although, this interpretation may have validity, it is apparently invalid in case of compensatory or most likely pathological sinus tachycardia, as shown in our experiments, in which sinus tachycardia in Hum*CHGA*19 in effect significantly reduced HF area. Therefore, we counter the notion that HF-QRS band power may somehow be positively related to HR under all circumstances. Our observation of reduced relative HF-band power in Hum*CHGA*19 is more synchronous with the published results of Bhargava et al. who evidenced in cardiac patients attenuation of HF-QRS power, with arrhythmogenicity [38].

It appears that the change in QTVI for Hum*CHGA*19 was contributed mainly by the reduction in HR variance (84 % over WT), whereas restitution toward normalcy of QTVI in Hum*CHGA*31 was primarily achieved via a big reduction in QTb variance (>73 % over WT). In Hum*CHGA*19 mice, QT duration was prolonged, QTb/PQ increased, and PQ conduction time decreased. These are indices of cardiomyopathy as proposed by Comi et al. in patients with Duchenne and Becker muscular dystrophy [39]. Shorter PQ interval and prolonged QTb interval with tachycardia may be the manifestation of relative sympatheticotonia. Moreover, changes in QRS HF characteristics in Hum*CHGA*19 suggest possible existence of ventricular enlargement, as suggested by Schlegel et al. [40]. It is concluded that previously reported hypertension in Hum*CHGA*19 alters autonomic modulation of their HR, ventricular depolarization, and repolarization profiles [21]. Clinically, heightened level of CHGA has been found in patients with CHF, MI, and LVH with consequent QT abnormality [41, 42]. However, this investigation proves that reduced CHGA/CST can also lead to QT prolongation and electrocardiographic features of LVH, suggesting that non-optimal (both low and high CHGA) can be responsible for the EKG characteristics mentioned. To this aspect, future strategy should focus on reducing hypertension using specific non-competitive nicotinic inhibitory agent such as CST natural variants [43]. Since optimal expression of CHGA by Hum*CHGA*31 ameliorates QT abnormality observed in Hum*CHGA*19, the conjecture that CHGA expression level plays a significant role is firmly established. The fate of QT status may depend on the proportional contribution by both CST fragment and full length CHGA. The CST region knockout mouse model could further reveal the intricacies involved in the seemingly paradoxical events. Observed EKG changes in Hum*CHGA*19 mice may just lower the threshold of ventricular susceptibility, increasing cardiovascular risk. Zhang et al. observed a unique relationship between CHGA level and survival rate in patients [44]. Their data indicate higher survival rate in patients with low CHGA in plasma. Whether such an observation is a direct link and applies to Hum*CHGA*19 mice is a mere gesture.

Experimental limitations The relation of the QT interval and HR is modified by a number of physiologic processes. The mechanism causing the change in HR may variably influence ventricular repolarization. Determination of the onset and the end of cardiac phenomena based on the partial view given by a single lead (in this case lead II) is intrinsically limited, as discussed by Malik and, therefore, may limit a robust interpretation quantitatively, without affecting the qualitative judgment [45]. However, it is not known if QT abnormality in Hum*CHGA*19 is mediated by the autonomic influences predominantly or by the non-autonomic pathway, e.g., exaggerated fractional shortening and consequent heavy ejection fraction loss. Also, the ionic current behavior for repolarization in mice is somewhat different from that of human. Therefore, drawing parallel between these species can be brought into question. We hypothesize that triggering of QTb prolongation at the low end of CHGA expression spectrum is most likely caused by autonomic dysfunction. However, the evidence in *Chga*−/− would substantially strengthen the argument albeit speculative in absence of direct evidence [15]. The findings of the present study demonstrate that BP increases observed in our earlier investigation affect ventricular repolarization status, along with changes in the depolarization properties [21]. In the face of elevated catecholamine secretion, finely regulated by the proportional contributions of circulating CHGA and catecholamine release inhibitory fragment, CST, QTb is prolonged. Future studies will involve delineating the mechanism by which the action potential duration at the level of ventricular myocytes is required to strengthen arguments concerning QT prolongation. Thus, our "humanized" *CHGA* mice are unique models to address the role of CHGA and CST in human cardiac electrical activity.

Acknowledgments This study was supported by grants from the National Institutes of Health—K01DK069613 and R01 HL108629 to Vaingankar, S.M. We would like to thank Professors O'Connor, D. T., Pajor A., Mahata, S. K., and Ahmad, H.R. for their critical input.

Disclosures The authors declare no conflicts of interest.

References

1. Taupenot, L., Harper, K. L., & O'Connor, D. T. (2003). The chromogranin-secretogranin family. *New England Journal of Medicine, 348*, 1134–1149.
2. Helle, K. B. (2000). The chromogranins. Historical perspectives. *Advances in Experimental Medicine and Biology, 482*, 3–20.
3. Iacangelo, A. L., & Eiden, L. E. (1995). Chromogranin A: current status as a precursor for bioactive peptides and a granulogenic/sorting factor in the regulated secretory pathway. *Regulatory Peptides, 58*, 65–88.
4. Mahapatra, N. R., Taupenot, L., Courel, M., Mahata, S. K., & O'Connor, D. T. (2008). The trans-Golgi proteins SCLIP and SCG10 interact with chromogranin A to regulate neuroendocrine secretion. *Biochemistry, 47*, 7167–7178.
5. Elias, S., Delestre, C., Ory, S., Marais, S., Courel, M., Vazquez-Martinez, R., et al. (2012). Chromogranin A induces the biogenesis of granules with calcium- and actin-dependent dynamics and exocytosis in constitutively secreting cells. *Endocrinology, 153*, 4444–4456.
6. Mahapatra, N. R., Mahata, M., Mahata, S. K., & O'Connor, D. T. (2006). The chromogranin A fragment catestatin: specificity, potency and mechanism to inhibit exocytotic secretion of multiple catecholamine storage vesicle co-transmitters. *Journal of Hypertension, 24*, 895–904.
7. Pasqua, T., Corti, A., Gentile, S., Pochini, L., Bianco, M., Metz-Boutigue, M. H., et al. (2013). Full-length human chromogranin-A cardioactivity: myocardial, coronary, and stimulus-induced processing evidence in normotensive and hypertensive male rat hearts. *Endocrinology, 154*, 3353–3365.
8. Penna, C., Alloatti, G., Gallo, M. P., Cerra, M. C., Levi, R., Tullio, F., et al. (2010). Catestatin improves post-ischemic left ventricular function and decreases ischemia/reperfusion injury in heart. *Cellular and Molecular Neurobiology, 30*, 1171–1179.
9. O'Connor, D. T., Takiyyuddin, M. A., Printz, M. P., Dinh, T. Q., Barbosa, J. A., Rozansky, D. J., et al. (1999). Catecholamine storage vesicle protein expression in genetic hypertension. *Blood Pressure, 8*, 285–295.
10. Takiyyuddin, M. A., Parmer, R. J., Kailasam, M. T., Cervenka, J. H., Kennedy, B., Ziegler, M. G., et al. (1995). Chromogranin A in human hypertension. Influence of heredity. *Hypertension, 26*, 213–220.
11. Kennedy, B. P., Mahata, S. K., O'Connor, D. T., & Ziegler, M. G. (1998). Mechanism of cardiovascular actions of the chromogranin A fragment catestatin in vivo. *Peptides, 19*, 1241–1248.
12. Mahata, S. K., Mahata, M., Livsey Taylor, C. V., Taupenot, L., Parmer, R. J., & O'Connor, D. T. (2000). The novel catecholamine release-inhibitory peptide catestatin (chromogranin A344-364). Properties and function. *Advances in Experimental Medicine and Biology, 482*, 263–277.
13. O'Connor, D. T., Kailasam, M. T., Kennedy, B. P., Ziegler, M. G., Yanaihara, N., & Parmer, R. J. (2002). Early decline in the catecholamine release-inhibitory peptide catestatin in humans at genetic risk of hypertension. *Journal of Hypertension, 20*, 1335–1345.
14. O'Connor, D. T., Zhu, G., Rao, F., Taupenot, L., Fung, M. M., Das, M., et al. (2008). Heritability and genome-wide linkage in US and Australian twins identify novel genomic regions controlling chromogranin a: implications for secretion and blood pressure. *Circulation, 118*, 247–257.
15. Gayen, J. R., Gu, Y., O'Connor, D. T., & Mahata, S. K. (2009). Global disturbances in autonomic function yield cardiovascular instability and hypertension in the chromogranin a null mouse. *Endocrinology, 150*, 5027–5035.
16. Mahapatra, N. R., O'Connor, D. T., Vaingankar, S. M., Hikim, A. P., Mahata, M., Ray, S., et al. (2005). Hypertension from targeted ablation of chromogranin A can be rescued by the human ortholog. *Journal of Clinical Investigation, 115*, 1942–1952.
17. Dev, N. B., Gayen, J. R., O'Connor, D. T., & Mahata, S. K. (2010). Chromogranin A and the autonomic system: decomposition of heart rate variability and rescue by its catestatin fragment. *Endocrinology, 151*, 2760–2768.
18. Meng, L., Wang, J., Ding, W., Han, P., Yang, Y., Qi, L., et al. (2013). Plasma catestatin level in patients with acute myocardial infarction and its correlation with ventricular remodelling. *Postgraduate Medical Journal, 89*, 193–196.
19. Puddu, P. E., Pasternac, A., Tubau, J. F., Krol, R., Farley, L., & Champlain, J. D. (1983). QT interval prolongation and increased plasma catecholamine levels in patients with mitral valve prolapse. *American Heart Journal, 105*, 422–428.
20. Algra, A., Tijssen, J. G., Roelandt, J. R., Pool, J., & Lubsen, J. (1991). QTc prolongation measured by standard 12-lead electrocardiography is an independent risk factor for sudden death due to cardiac arrest. *Circulation, 83*, 188–194.
21. Vaingankar, S. M., Li, Y., Corti, A., Biswas, N., Gayen, J., O'Connor, D. T., et al. (2010). Long human CHGA flanking chromosome 14 sequence required for optimal BAC transgenic "rescue" of disease phenotypes in the mouse Chga knockout. *Physiological Genomics, 41*, 91–101.
22. Steare, S. E., Dubowitz, V., & Benatar, A. (1992). Subclinical cardiomyopathy in Becker muscular dystrophy. *British Heart Journal, 68*, 304–308.
23. Mir, S. A., Chatterjee, A., Mitra, A., Pathak, K., Mahata, S. K., & Sarkar, S. (2012). Inhibition of signal transducer and activator of transcription 3 (STAT3) attenuates interleukin-6 (IL-6)-induced collagen synthesis and resultant hypertrophy in rat heart. *The Journal of Biological Chemistry, 287*, 2666–2677.
24. Sen, S., Tarazi, R. C., Khairallah, P. A., & Bumpus, F. M. (1974). Cardiac hypertrophy in spontaneously hypertensive rats. *Circulation Research, 35*, 775–781.
25. Bazett, H. C. (1920). An analysis of time relations of electrocardiogram. *Heart, 7*, 53–70.
26. Decher, N., Wemhoner, K., Rinne, S., Netter, M. F., Zuzarte, M., Aller, M. I., et al. (2011). Knock-out of the potassium channel TASK-1 leads to a prolonged QT interval and a disturbed QRS complex. *Cellular Physiology and Biochemistry, 28*, 77–86.
27. Mitchell, G. F., Jeron, A., & Koren, G. (1998). Measurement of heart rate and Q-T interval in the conscious mouse. *The American Journal of Physiology, 274*, H747–H751.
28. Berger, R. D., Kasper, E. K., Baughman, K. L., Marban, E., Calkins, H., & Tomaselli, G. F. (1997). Beat-to-beat QT interval variability. *Circulation, 96*, 1557–1565.
29. Xing, S., Tsaih, S. W., Yuan, R., Svenson, K. L., Jorgenson, L. M., So, M., et al. (2009). Genetic influence on electrocardiogram time intervals and heart rate in aging mice. *American Journal of Physiology. Heart and Circulatory Physiology, 296*, H1907–H1913.
30. Atterhog, J. H., & Loogna, E. (1977). PR interval in relation to heart rate during exercise and the influence of posture and autonomic tone. *Journal of Electrocardiology, 10*, 331–336.
31. VanderBrink, B. A., Link, M. S., Aronovitz, M. J., Saba, S., Sloa, S. B., Homoud, M. K., et al. (1999). Assessment of atrioventricular nodal physiology in the mouse. *Journal of Interventional Cardiac Electrophysiology, 3*, 207–212.
32. Wang, X. J., & Ai, H. B. (1999). Studies on the relativity of power spectrum of QRS complex with heart rate, duration of QRS and Vp-p of QRS. *Shandog J Biomed Eng, 18*, 32–38.
33. Vaingankar, S. M., Li, Y., Biswas, N., Gayen, J., Choksi, S., Rao, F., et al. (2010). Effects of chromogranin A deficiency and excess in vivo: biphasic blood pressure and catecholamine responses. *Journal of Hypertension, 28*, 817–825.
34. Extramiana, F., Tavernier, R., Maison-Blanche, P., Neyroud, N., Jordaens, L., Leenhardt, A., et al. (2000). Ventricular repolarization and Holter monitoring. Effect of sympathetic blockage on the QT/RR

ratio. *Archives des Maladies du Coeur et des Vaisseaux, 93*, 1277–1283.
35. Holt, J. H., Barnard, A. C. L., & Lynn, M. S. (1969). A study of the human heart as a multiple dipole electrical source. II. Diagnosis and quantification of left ventricular hypertrophy. *Circulation, 40*, 697–710.
36. Dunn, F. G., Pfeffer, M. A., & Frolich, E. D. (1978). ECG alterations with progressive left ventricular hypertrophy in spontaneous hypertension. *Clinical and Experimental Hypertension, 1*, 67–86.
37. Oikarinen, L., Nieminen, M. S., Viitasalo, M., Toivonen, L., Wachtell, K., Papademetriou, V., et al. (2001). Relation of QT interval and QT dispersion to echocardiographic left ventricular hypertrophy and geometric pattern in hypertensive patients. The LIFE study. The Losartan Intervention For Endpoint Reduction. *Journal of Hypertension, 19*, 1883–1891.
38. Bhargava, V., & Goldberger, A. (1981). Myocardial infarction diminishes both low and high frequency QRS potentials: power spectrum analysis of lead II. *Journal of Electrocardiology, 14*, 57–60.
39. Comi, L. I., Nigro, G., Politano, L., & Petretta, V. R. (1992). The cardiomyopathy of Duchenne/Becker consultants. *International Journal of Cardiology, 34*, 297–305.
40. Schlegel, T. T. K. W., DePalma, J. L., Feiveson, A. H., Wilson, J. S., Rahman, M. A., & Bungo, M. W. (2004). Real-time 12-lead high-frequency QRS electrocardiography for enhanced detection of myocardial ischemia and coronary artery disease. *Mayo Clinic Proceedings, 79*, 339–350.
41. Ceconi, C., Ferrari, R., Bachetti, T., Opasic, C., Volterrani, M., Colombo, B., et al. (2002). Chromogranin A in heart failure; a novel neurohumoral factor and a predictor for mortality. *European Heart Journal, 23*, 967–974.
42. Omland, T., Dickstein, K., & Syversen, U. (2003). Association between plasma chromogranin A concentration and long-term mortality after myocardial infarction. *American Journal of Medicine, 114*, 25–30.
43. Mahata, S. K., Mahata, M., Fung, M. M., & O'Connor, D. T. (2010). Catestatin: a multifunctional peptide from chromogranin A. *Regulatory Peptides, 165*, 52–62.
44. Zhang, D., Lavaux, T., Voegeli, A. C., Lavigne, T., Castelain, V., Meyer, N., et al. (2008). Prognostic value of chromogranin A at admission in critically ill patients: a cohort study in a medical intensive care unit. *Clinical Chemistry, 54*, 1947–1503.
45. Malik, M. (2004). Errors and misconceptions in ECG measurement used for the detection of drug induced QT-interval prolongation. *Journal of Electrocardiology, 37*, 25–33A.